

Chemical Stability and Biological Properties of Plasma-Sprayed CaO-SiO₂-ZrO₂ Coatings

Ying Liang, Youtao Xie, Heng Ji, Liping Huang, and Xuebin Zheng

(Submitted January 27, 2010; in revised form May 22, 2010)

In this work, calcia-stabilized zirconia powders were coated by silica derived from tetraethoxysilane (TEOS) hydrolysis. After calcining at 1400 °C, decalcification of calcia-stabilized zirconia by silica occurred and powders composed of Ca₂SiO₄, ZrO₂, and CaZrO₃ were prepared. We produced three kinds of powders with different Ca₂SiO₄ contents [20 wt.% (denoted as CZS2), 40 wt.% (denoted as CZS4), and 60 wt.% (denoted as CZS6)]. The obtained powders were sprayed onto Ti-6Al-4V substrates using atmospheric plasma spraying. The microstructure of the powders and coatings were analyzed. The dissolution rates of the coatings were assessed by monitoring the ions release and mass losses after immersion in Tris-HCl buffer solution. Results showed that the chemical stability of the coatings were significantly improved compared with pure calcium silicate coatings, and increased with the increase of Zr contents. The CZS4 coating showed not only good apatite-formation ability in simulated body fluid, but also well attachment and proliferation capability for the canine bone marrow stem cells. Results presented here indicate that plasma-sprayed CZS4 coating has medium dissolution rate and good biological properties, suggesting its potential use as bone implants.

Keywords atmospheric plasma spraying, biological properties, CaO-SiO₂-ZrO₂, chemical stability, core-shell structure, TEOS hydrolysis

1. Introduction

Plasma-sprayed hydroxyapatite (HA) and titanium coatings on Ti-6Al-4V substrates have been widely used in orthopedics and dentistry (Ref 1-3). However, HA tends to decompose during plasma-spraying process, into ancillary bioresorbable phases such as tricalcium phosphate (TCP), tetracalcium phosphate (TTCP), which reduces the physiological stability of HA. Furthermore, brittleness and poor bonding strength of HA coating always result in rapid wear, peeling, and premature fracture of the coated layer (Ref 4-7). Titanium coating is bioinert, which cannot bond directly to living bone as bioactive HA can (Ref 8).

Since Hench and Anderson (Ref 9) found bioglass in 1969, several glasses and glass ceramics were introduced as bioactive materials which could directly bond to living bone in human body through the apatite layer formed on

This article is an invited paper selected from presentations at the 4th Asian Thermal Spray Conference (ATSC 2009) and has been expanded from the original presentation. ATSC 2009 was held at Nanyang Hotel, Xi'an Jiaotong University, Xi'an, China, October 22-24, 2009, and was chaired by Chang-Jiu Li.

Ying Liang, Youtao Xie, Heng Ji, Liping Huang, and Xuebin Zheng, Key Laboratory of Inorganic Coating Materials, Chinese Academy of Science, 1295 Dingxi Road, Shanghai 200050, China and Shanghai Institute of Ceramics, Chinese Academy of Science, 1295 Dingxi Road, Shanghai 200050, China. Contact e-mails: yliang@student.sic.ac.cn and xbzheng@mail.sic.ac.cn.

the implants (Ref 10). Kokubo (Ref 11) pointed that CaO-SiO₂ component in those materials mainly contributes to their bioactivity. Hence in the past two decades, CaO-SiO₂ based ceramics have received great attentions as potential bioactive materials for bone tissue regeneration (Ref 12, 13). Thermally sprayed bioglass coatings were not studied widely due to their vaporization during the spraying process and poor bond strength with titanium substrate (Ref 14). Plasma-sprayed calcium silicate coating exhibits good bond strength and apatite-formation ability (Ref 15). However, major drawback of the CaO-SiO₂ based ceramic coatings is their high dissolution rate, and therefore leading to deterioration of the mechanical properties of the coatings and a high pH value in the surrounding environment, which is detrimental to the vicinal cells (Ref 16-18).

Zirconia-based ceramics are widely used because of their mechanical properties and biocompatibility in the human body (Ref 19, 20). Zirconia is also used to reinforce biomedical coatings due to the excellent stability (Ref 21, 22). However, zirconia reinforced coatings are mostly fabricated by spraying powders simply prepared by mixing via ball milling; the nonuniformity of coatings' microstructure would still cause the degradation and failure of the coatings. Colin et al. (Ref 23) found that calcia-stabilized zirconia may react with acid oxide such as silica at high temperature, forming a calcium silicate contained layer coated on the zirconia particles. Such a core-shell structure may help in stabilizing the microstructure of the coatings. When the "shell" (calcium silicate) dissolves fastly in physiological environment, the residual "core" (calcia-stabilized zirconia) would still connect in a network to prevent the fracture of the coatings. In this study, we coated SiO₂ on calcia-stabilized zirconia particles uniformly by TEOS hydrolysis method. After sintering

at high temperature, $\text{CaO}\text{-SiO}_2\text{-ZrO}_2$ powders having core-shell structure were prepared. The corresponding coatings were deposited by atmospheric plasma-spraying system. The objective of the present study was to improve the chemical stability of the coatings by incorporating ZrO_2 into $\text{CaO}\text{-SiO}_2$ system and to investigate the biological properties of the $\text{CaO}\text{-SiO}_2\text{-ZrO}_2$ coatings.

2. Materials and Methods

2.1 Powders Preparation and Plasma Spraying

The raw materials used in this study were commercially available ZrO_2 powders, CaCO_3 (A.R.) and TEOS ($(\text{C}_2\text{H}_5\text{O})_4\text{Si}$, A.R.). Powders with different theoretical content of Ca_2SiO_4 (20, 40, and 60 wt.%) in the end products were prepared, denoted as CZS2, CZS4, and CZS6. The composition of the powders was to be designed based on the $\text{CaO}\text{-ZrO}_2\text{-SiO}_2$ (CZS) melting phase diagram (Ref 24). Each composition is listed in Table 1, which is theoretically calculated based on the different composition ratio (mol.%) within the triangle $\text{Ca}_2\text{SiO}_4\text{-ZrO}_2\text{-CaZrO}_3$ of the phase diagram of CZS (Fig. 1).

ZrO_2 powders mechanically mixed with CaCO_3 were heated to 1400 °C in alumina crucible in a box-type furnace. The reaction lasted for 6 h in air and the powders were slowly furnace-cooled to room temperature. The acquired calcia-stabilized zirconia powders were suspended in ethanol, and then H_2O and NH_3 were added. To prevent the rapid hydrolysis of TEOS and independent nucleation of SiO_2 , TEOS were added drop by drop (mol ratio: TEOS/ $\text{H}_2\text{O}/\text{NH}_3 = 1:40:3$). The reaction lasted for 10 h at 50 °C under stirring. Then, the suspend solution was filtrated, dried, and finally calcined according to the same procedure as the calcia-stabilized zirconia.

Ti-6Al-4V substrates with dimensions of 10 mm × 10 mm × 2 mm were ultrasonically cleaned in ethanol and grit-blasted with alumina grit before plasma spraying. An atmospheric plasma-spraying system (F4-MB, Sulzer Metco, Switzerland) was applied to fabricate the coatings. Table 2 lists the parameters for plasma spraying of the powders.

2.2 Characterization of the Powders and Coatings

The crystalline phases of the powders and coatings were analyzed by x-ray diffraction (XRD, *D/max* 2550 V, Rigaku, Japan), using $\text{Cu K}\alpha$ radiation at 40 kV and 100 mA. The microstructure of the powders and coatings were evaluated by electron probe micro-analyzer (EPMA,

JXA-8100, JEOL, Japan) and field emission scanning electron microscope (FE-SEM, JSM-6700F, JEOL, Japan). The morphology of the CZS4 powder was also investigated by transmission electron microscopy (TEM, JEM-2010, JEOL, Japan). Energy dispersive spectrometer (EDS, INCA ENERGY, UK) was performed to identify the compositions of the powders. Average surface roughness (R_a) of the coatings was measured by surface test apparatus (T8000, Hommel werke, Germany). Two specimens of each coating were used for test and each specimen was measured ten times at different test area.

2.3 Chemical Stability in Tris-HCl Buffer Solution

Each sample was immersed in 50 mL Tris-HCl buffer solution for the dissolution behavior test. The Tris-HCl solution was prepared by dissolving 50 mM Tris(hydroxymethyl)aminomethane ($(\text{CH}_2\text{OH})_3\text{CNH}_2$) in deionized water and then buffered at pH 7.40 with hydrochloric acid (HCl) at 37 °C. The volume of the solutions kept constant as 50 mL during the immersion, and the samples were placed in the solutions without agitation. The ratio of surface area (mm^2)/volume (mL) was 2. After immersion for 14 days, there was not any precipitation in the solutions. The mass losses of the coatings were measured. The Ca, Si, and Zr ion

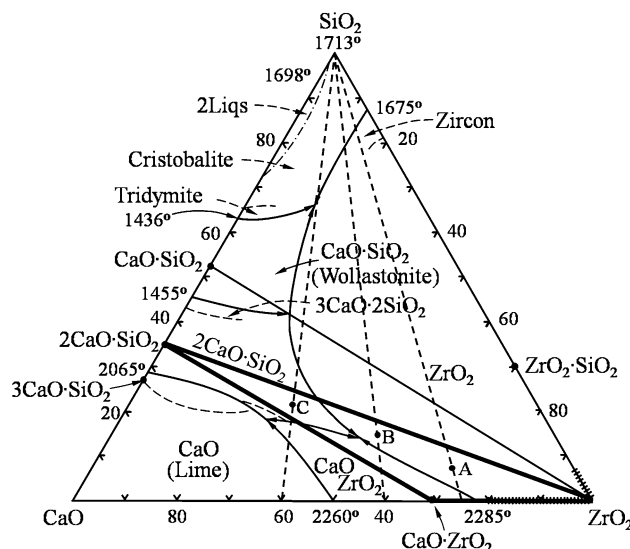


Fig. 1 Composition in the $\text{CaO}\text{-ZrO}_2\text{-SiO}_2$ phase diagram. A, B, and C denote CZS2, CZS4, and CZS6, respectively

Table 2 Plasma-spraying parameters

Argon plasma gas flow rate, slpm	40
Hydrogen plasma gas flow rate, slpm	10
Spray distance, mm	100
Argon powder carrier gas, slpm	3.5
Current, A	650
Voltage, V	68
Powder feed rate, g/min	25
Slpm, Standard liter per minute	

Table 1 Chemical composition of raw materials (mol.%)

Samples	CaO	ZrO ₂	TEOS (SiO ₂)
CZS2	37.81	51.57	10.62
CZS4	48.48	33.10	18.42
CZS6	58.24	17.68	24.08

concentration in Tris-HCl solutions were determined by inductively coupled plasma atomic emission spectroscopy (ICP-AES, VistaAX, Varian, USA). Ca_2SiO_4 coating was tested in the same condition as a contrast. The pH value changes of the solutions after 7 days immersion were tested by a pH meter (Spsic, China).

2.4 Apatite-Formation Ability of As-Sprayed Coatings in Simulated Body Fluid

Simulated body fluids (SBF) is composed of 142.0 mM Na^+ , 5.0 mM K^+ , 1.5 mM Mg^{2+} , 2.5 mM Ca^{2+} , 147.8 mM Cl^- , 4.2 mM HCO_3^- , 1.0 mM HPO_4^{2-} , and 0.5 mM SO_4^{2-} , which has similar ion concentrations to human blood plasma. SBF is always used to evaluate the apatite-formation ability of materials (Ref 25). The specimens were soaked in SBF at 37 °C for 1 week. The soaked coatings were dried and coated with carbon before SEM and EDS analysis.

2.5 Cell Culture

Canine bone marrow stem cells (MSCs) were used to evaluate the cytocompatibility of the CZS4 coating. Cells were suspended in 200 μL Dulbecco's modified Eagle's medium, containing 10% (v/v) fetal bovine serum, 100 U/mL penicillin, and 100 mg/mL streptomycin. Cell suspension with a density of 5×10^4 cells/mL was seeded onto the coating surface for 2, 4, and 6 days. At the end of each time point, samples were fixed with 2.5% glutaraldehyde in sodium cacodylate buffer (pH 7.4), followed by sequential dehydration in graded ethanol (50%, 70%, 95%, and 100%) before SEM observation.

3. Results and Discussion

3.1 Characterization of Powders and Coatings

The XRD patterns of the obtained powders and coatings are shown in Fig. 2. The powders were mainly composed of miscellaneous amounts of $\gamma\text{-Ca}_2\text{SiO}_4$, ZrO_2 (cubic/tetragonal), and CaZrO_3 (Fig. 2a), which was in consistent with the CZS phase diagram. ZrO_2 and CaZrO_3 were main phases in CZS2 powder, while Ca_2SiO_4 peaks were relatively weak. The intensity of Ca_2SiO_4 peaks increased, and there was still a majority of ZrO_2 and CaZrO_3 phases in CZS4 powder. CZS6 powder had the most intensive Ca_2SiO_4 peaks, with increasing CaO and decreasing ZrO_2 content in the raw materials, more CaZrO_3 was formed, ZrO_2 peaks were not quite detectable.

CaZrO_3 was one of the main phases in the CZS powders, therefore as a biomaterial its biocompatibility needed to be considered. Uetsuji et al. (Ref 26) found that CaZrO_3 showed no cytotoxicity when fibroblast (L929) cells were cultured on it, indicating that it is biocompatible in a physiological environment.

During the plasma-spraying process, the crystallinity of materials decreased due to rapid melting and re-solidification, as shown in Fig. 2(b). The Ca_2SiO_4 peaks could hardly be

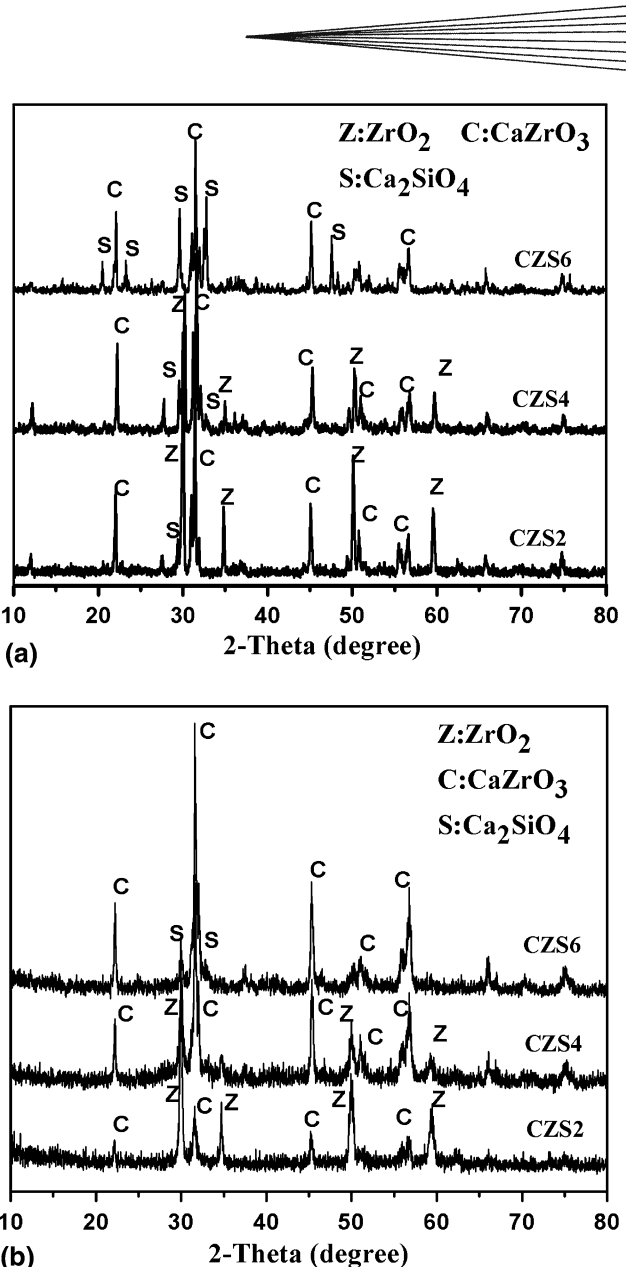


Fig. 2 XRD patterns of (a) $\text{CaO}\text{-}\text{ZrO}_2\text{-}\text{SiO}_2$ powders and (b) as-sprayed coatings

observed in the XRD spectra because the peaks intensity of ZrO_2 and CaZrO_3 were much higher than that of Ca_2SiO_4 . Besides, no monoclinic zirconia was found in the sprayed coatings, which indicated that no ZrO_2 transformed in the process. The surface roughness (Ra) of each coating was $6.67 \pm 0.61 \mu\text{m}$, $5.32 \pm 0.59 \mu\text{m}$, and $6.43 \pm 0.65 \mu\text{m}$, respectively.

The morphology of the obtained powders is shown in Fig. 3. On the whole, there was no obvious separate phases of Ca_2SiO_4 , ZrO_2 , or CaZrO_3 . During the first process that calcia-stabilized zirconia was prepared, CaZrO_3 formed due to high CaO content in the three compositions (Ref 27). Then, the particles were coated uniformly by SiO_2 layer derived from the hydrolysis of TEOS. At high temperature, driven by the formation of

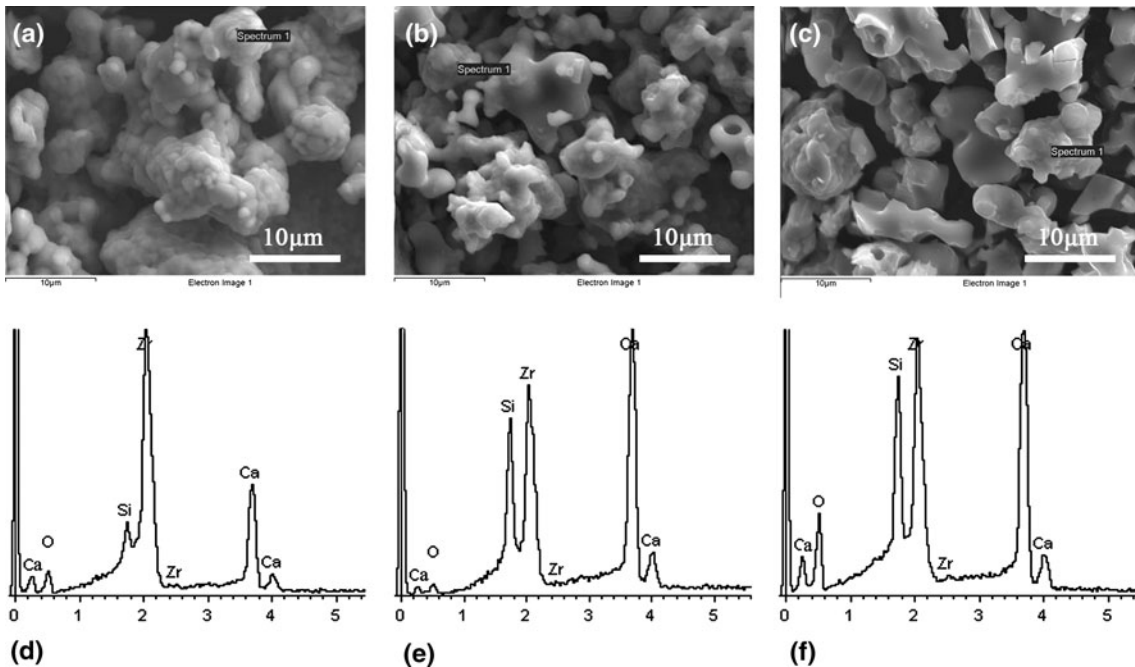


Fig. 3 SEM micrographs of the $\text{CaO-ZrO}_2\text{-SiO}_2$ powders: (a) CZS2, (b) CZS4, (c) CZS6, (d) EDS spectrum of (a), (e) EDS spectrum of (b), and (f) EDS spectrum of (c)

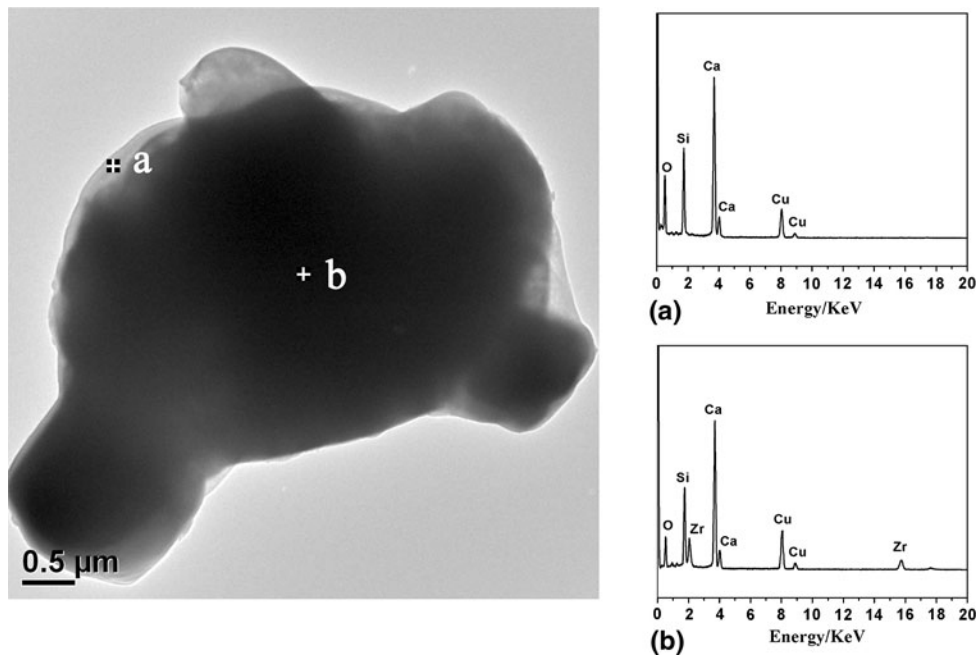


Fig. 4 TEM micrograph of the CZS4 powders and EDS analysis

calcium silicate, CaO was extracted from the zirconia matrix, diffused into the SiO_2 layer, and reacted to form silicates layer (Ref 23). EDS analysis reveals that the particles contained Si, and based on the mechanism of decalcification and XRD result we can speculate that the $\text{ZrO}_2/\text{CaZrO}_3$ particles were coated by a thin layer of Ca_2SiO_4 . Figure 4 further confirmed that in the modified

CZS4 powder, the particles have the core-shell structure. The EDS analysis suggests that the $\text{ZrO}_2/\text{CaZrO}_3$ particle was coated by calcium silicate. $\text{ZrO}_2/\text{CaZrO}_3$ central nucleus played the role of built-in stabilization, and a layer of Ca_2SiO_4 on the “nucleus” ensured the bioactivity of the materials. After implanted into the animal body, the Ca_2SiO_4 in the coatings dissolves, while the $\text{ZrO}_2/\text{CaZrO}_3$

particles could still connect in a network to maintain the mechanical properties of the coatings.

3.2 Chemical Stability of the Coatings in Tris-HCl Buffer Solution

ICP-AES analysis demonstrates much lower release of Ca and Si ions when CZS2, CZS4, and CZS6 coatings were immersed in Tris-HCl buffer solution compared with Ca_2SiO_4 (Fig. 5a and b). The Ca and Si ions release of the Ca_2SiO_4 coating were the highest and reached 7.604 ± 0.601 and 2.294 ± 0.083 mM after 14 days immersion. Same was true for mass losses of the coatings, as shown in Fig. 5(c). It can be seen that the dissolution rates decreased with increase of Zr contents in the coatings. The Ca and Si ions concentration of CZS6 coating after soaking in Tris-HCl buffer solution for 14 days were 4.847 ± 0.164 and 1.010 ± 0.022 mM, respectively. However, while in CZS2, Zr contents increased by two times, the concentration of Ca and Si ions decreased to 0.646 ± 0.035 and 0.131 ± 0.007 mM. No Zr ions was detected in the Tris-HCl solutions for all the three coatings due to its high stability.

The pH value changes of the solutions after 7 days immersion were listed in Table 3. During the immersion, Ca^{2+} of the coatings exchanged with H^+ in the solution and therefore leading to increase of the pH value. The pH values of the solutions were CZS6 > CZS4 > CZS2, which were consistent with the Ca^{2+} releases of the three coatings. It can be seen that CZS2, CZS4, and CZS6 coatings possessed a significantly lower ionic release rate and mass losses than Ca_2SiO_4 coating, and this effect directly correlated to Zr contents, suggesting that Zr plays an important part in modulating the chemical stability of the coatings.

3.3 Apatite Formation on As-Sprayed Coatings in SBF

The morphologies of the as-sprayed coatings are shown in Fig. 6(a), (c), and (e). There is no obvious difference among the three coatings, which were developed from melted and half-melted splats with a rough and uneven surface. After soaking in SBF for 7 days, there is no distinct change in the surface view of CZS2 coating, as shown in Fig. 6(b). EDS analysis of the coating surface showed that it was composed of Ca, Zr, Si, and O, which were derived from the original powder. No apatite was formed on the CZS2 coating. However, new apatite layers formation were obvious on the CZS4 and CZS6 coatings after soaking in SBF for 7 days (Fig. 6d and f), which were confirmed by the corresponding EDS spectra.

Ca_2SiO_4 coating is known to be bioactive and can bond with bone through the formation of an apatite layer on its surface (Ref 15). Incorporating Zr into Ca-Si system decreased the dissolution of Ca and Si ions, yet it did not inhibit the apatite-formation ability in SBF when Ca_2SiO_4 contents were more than 40 wt. %.

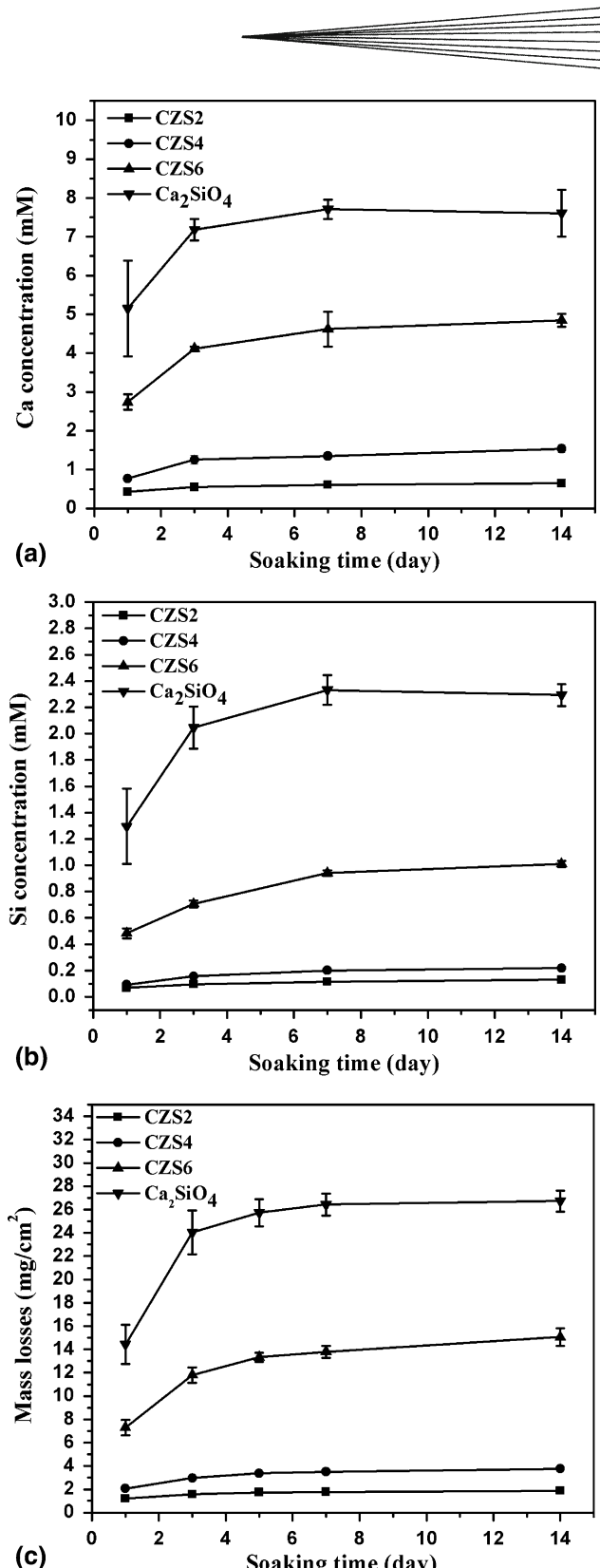


Fig. 5 The change of ions concentration in Tris-HCl buffer solution and mass losses of the coatings after soaking for 14 days. (a) Ca ions, (b) Si ions, and (c) mass losses

3.4 Morphology of Cells on As-Sprayed Coatings

Cell adhesion plays an important role in cell growth and proliferation. The morphology of canine bone MSCs seeded on the CZS4 coating for various times is presented in Fig. 7. The morphology of the cells was similar to

Table 3 The pH value changes of the Tris-HCl solution after 7 days immersion

Samples	pH value (before immersion)	pH value (after 7 days immersion)
CZS2	7.40	7.53
CZS4	7.40	7.66
CZS6	7.40	7.83

spindle shape. After 4 days culture, the cells grew and spread well with characteristic filopodia-like projections on the coating surface. After 6 days culture, the cells reached confluence and formed a sheet-layer on the coating surface. It can be seen that the CaO-SiO₂-ZrO₂ coatings supported the adhesion and proliferation of MSCs. There was no indication that incorporating zirconium into Ca-Si system induced cytotoxicity.

4. Conclusion

CaO-ZrO₂-SiO₂ coatings with different Ca₂SiO₄ contents were fabricated on titanium alloy substrates by atmospheric plasma spraying. The feedstocks were synthesized by sintering silica-coated calcia-stabilized zir-

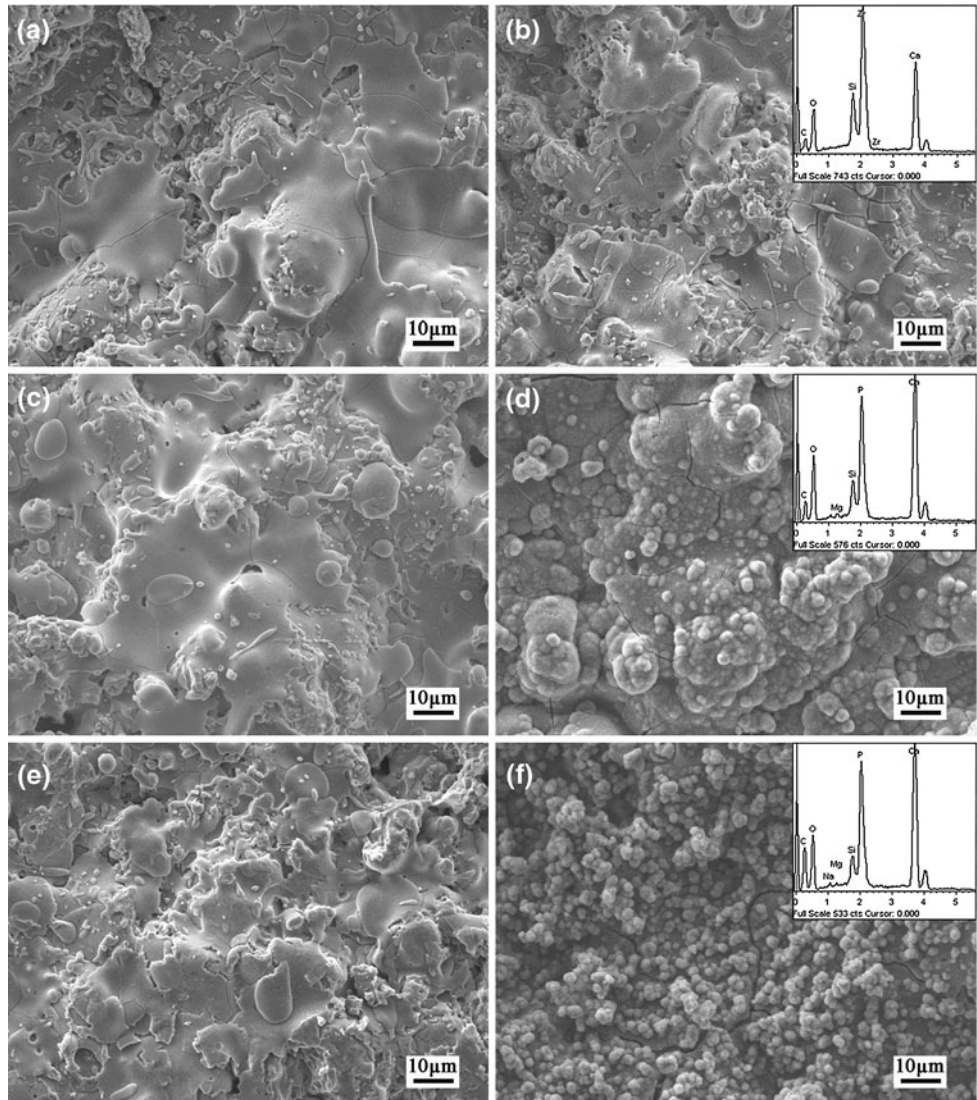


Fig. 6 SEM micrographs of CZS2, CZS4, and CZS6 coatings before and after soaking in SBF for 7 days. (a) CZS2 before and (b) after soaking, (c) CZS4 before and (d) after soaking, (e) CZS6 before, and (f) after soaking (insets are EDS spectra)

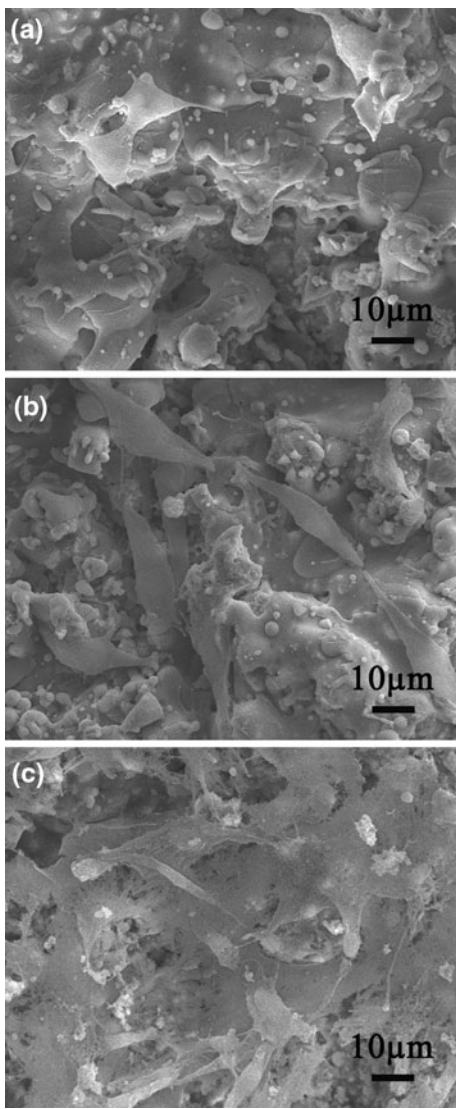


Fig. 7 SEM morphologies of the MSCs on the CZS4 coating after various times of culture: (a) 2 days, (b) 4 days, and (c) 6 days

conia powders at 1400 °C. The prepared powders were mainly composed of ZrO_2 , $CaZrO_3$, and Ca_2SiO_4 . The particles possessed a core-shell structure in which ZrO_2 / $CaZrO_3$ play the part of nucleus and Ca_2SiO_4 layer was coated on the $ZrO_2/ CaZrO_3$ nucleus. Incorporating Zr into Ca-Si system significantly increased the chemical stability of the coatings compared with Ca_2SiO_4 , and with the increase of Zr contents, the dissolution rates of the coatings decreased. The CZS4 and CZS6 coatings exhibited good apatite-formation ability in SBF, which did not inhibited by Zr incorporation. The in vitro cell culture showed that canine bone MSCs could adhere and proliferate well on the CZS4 coating surface. The CZS4 coating with medium dissolution rate and good biological properties might have potential use as bone/dental implants.

References

1. L.L. Hench, Bioceramics, *J. Am. Ceram. Soc.*, 1998, **81**, p 1705-1728
2. G.L. Darimont, R. Cloots, E. Heinen, L. Seidel, and R. Legrand, In Vivo Behaviour of Hydroxyapatite Coatings on Titanium Implants: A Quantitative Study in the Rabbit, *Biomaterials*, 2002, **23**, p 2569-2575
3. W.C. Xue, X.Y. Liu, X.B. Zheng, and C.X. Ding, In Vivo Evaluation of Plasma-Sprayed Titanium Coating after Alkali Modification, *Biomaterials*, 2005, **26**, p 3029-3037
4. X.B. Zheng and C.X. Ding, Study on Plasma Sprayed HA/Ti Composite Coating. I. Microstructure, Phase Composition and Mechanical Properties, *J. Inorg. Mater.*, 2000, **15**, p 897-902
5. Y.C. Tsui, C. Doyle, and T.W. Clyne, Plasma Sprayed Hydroxyapatite Coatings on Titanium Substrates. Part 1: Mechanical Properties and Residual Stress Levels, *Biomaterials*, 1998, **19**, p 2015-2029
6. Y.C. Tsui, C. Doyle, and T.W. Clyne, Plasma Sprayed Hydroxyapatite Coatings on Titanium Substrates. Part 2: Optimization of Coating Properties, *Biomaterials*, 1998, **19**, p 2031-2043
7. B.C. Wang, T.M. Lee, E. Chang, and C.Y. Yang, The Shear Strength and the Failure Mode of Plasma-sprayed Hydroxyapatite Coating to Bone: The Effect of Coating Thickness, *J. Biomed. Mater. Res.*, 1993, **27**, p 1315-1327
8. M. Wei, H.M. Kim, T. Kokubo, and J.H. Evans, Optimising the Bioactivity of Alkaline-Treated Titanium Alloy, *Mater. Sci. Eng. C*, 2002, **20**, p 125-134
9. L. Hench and O. Anderson, Bioactive Glass, *An Introduction to Bioceramics*, L. Hench and L. Wilson, Ed., World Scientific, USA, 1993, p 41
10. T. Nakamura, T. Yamamoto, S. Higashi, T. Kokubo, and S. Ito, A New Glass-Ceramic for Bone-Replacement-Evaluation of Its Bonding to Bone Tissue, *J. Biomed. Mater. Res.*, 1985, **19**, p 685-698
11. T. Kokubo, Surface-Chemistry of Bioactive Glass Ceramics, *J. Non-crystall. Solids*, 1990, **120**, p 138-151
12. P.N. De Aza, J.M. Fernandez-Pradas, and P. Serra, In Vitro Bioactivity of Laser Ablation Pseudowollastonite Coating, *Biomaterials*, 2004, **25**, p 1983-1990
13. S. Ni, J. Chang, L. Chou, and W. Zhai, Comparison of Osteoblast-Like Cell Responses to Calcium Silicate and Tricalcium Phosphate Ceramics In Vitro, *J. Biomed. Mater. Res. B*, 2007, **80**, p 174-183
14. G. Goller, The Effect of Bond Coat on Mechanical Properties of Plasma Sprayed Bioglass-Titanium Coatings, *Ceram. Int.*, 2004, **30**, p 351-355
15. X.Y. Liu, S.Y. Tao, and C.X. Ding, Bioactivity of Plasma Sprayed Dicalcium Silicate Coatings, *Biomaterials*, 2002, **23**, p 963-968
16. P. Siriphannon, Y. Kameshima, A. Yasumori, K. Okada, and S. Hayashi, Formation of Hydroxyapatite on $CaSiO_3$ Powders in Simulated Body Fluid, *J. Eur. Ceram. Soc.*, 2002, **22**, p 511-520
17. C. Wu, Y. Ramaswamy, A. Soeparto, and H. Zreiqat, Incorporation of Titanium into Calcium Silicate Improved Their Chemical and Biological Properties, *J. Biomed. Mater. Res. A*, 2008, **86**, p 402-410
18. Y. Ramaswamy, C. Wu, A. Van Hummel, V. Combes, G. Grau, and H. Zreiqat, The Responses of Osteoblasts, Osteoclasts and Endothelial Cells to Zirconium Modified Calcium-Silicate-Based Ceramics, *Biomaterials*, 2008, **29**, p 4392-4402
19. I. Dion, L. Bordenave, F. Lefebvre, R. Bareille, C. Baquey, R. Monties, and P. Havlik, Physico-Chemistry and Cytotoxicity of Ceramics, *J. Mater. Sci.*, 1994, **5**, p 18-24
20. G. Maccauro, N. Specchia, M. Arena, C. Piconi, and F. Greco, Biological Response to Calcia-partially Stabilized Zirconia Ceramics, *Proc. 8th ESB Meeting*, Roma, Italia, 1992, p 110
21. T. Kasuga, M. Yoshida, A.J. Ikushima, M. Tuchiya, and H. Kusakari, Stability of Zirconia-Toughened Bioactive Glass-Ceramics: In Vivo Study Using Dogs, *J. Mater. Sci. Mater. Med.*, 1993, **4**, p 36-39
22. Y.T. Xie, X.Y. Liu, X.B. Zheng, C.X. Ding, and P.K. Chu, Improved Stability of Plasma-Sprayed Dicalcium Silicate/Zirconia Composite Coating, *Thin Solid Films*, 2006, **515**, p 1214-1218

23. S. Colin, B. Dupre, and C. Gleitzer, Decalcification of Stabilized Zirconia by Silica and Some Other Oxides, *J. Eur. Ceram. Soc.*, 1992, **9**, p 389-395
24. K. Matsumoto, T. Sawamoto, and S. Koide, Fig. 664, *Phase Diagram for Ceramists*, M.K. Reser, Ed., Am. Ceram. Soc., Columbus, OH, 1964, p 231
25. T. Kokubo, H. Kushitani, C. Ohtsuki, S. Sakka, and T. Yamamuro, Chemical-Reaction of Bioactive Glass and Glass-Ceramics with a Simulated Body-Fluid, *J. Mater. Sci. Mater. Med.*, 1992, **3**, p 79-83
26. Y. Uetsuji, S. Fujimoto, K. Tsuchiya, and Y. Hirano, Cytotoxicity of Piezoelectric Materials in Colony Formation Assay, *J. Soc. Mater. Sci. Jpn.*, 2009, **58**, p 943-947
27. G.C. Wang, X.Y. Liu, and C.X. Ding, Phase Composition and In Vitro Bioactivity of Plasma Sprayed Calcia Stabilized Zirconia Coatings, *Surf. Coat. Technol.*, 2008, **202**, p 5824-5831